

# A proposal for a generation of two-color ultra-short x-ray pulses\*

Alexander Zholents

*Advanced Photon Source, Argonne National Laboratory  
Argonne, IL 60439*

The submitted manuscript has been created by UChicago Argonne, LLC, Operator of Argonne National Laboratory ("Argonne"). Argonne, a U.S. Department of Energy Office of Science laboratory, is operated under Contract No. DE-AC02-06CH11357. The U.S. Government retains for itself, and others acting on its behalf, a paid-up nonexclusive, irrevocable worldwide license in said article to reproduce, prepare derivative works, distribute copies to the public, and perform publicly and display publicly, by or on behalf of the Government.

---

\*Work supported by the U. S. Department of Energy, Office of Science, under Contract No. DE-AC02-06CH11357.

# A proposal for a generation of two-color ultra-short x- ray pulses

---

NGLS Technical Note 25

**Alexander Zholents**  
Argonne National Laboratory  
14 August 2012

## **Table of Contents**

I. Introduction	3
II. Method	3
III. Test Opportunity at LCLS	8
IV. Conclusion	9

## I. Introduction

Generation of two sub-femtosecond x-ray pulses with different and adjustable photon energies using a single electron bunch was considered in [1] for x-ray pump and x-ray probe experiments with a variable time delay between the first and the second x-ray pulses. A combination of the echo-enabled harmonic generation (EEHG) technique [2] and the current enhanced self-amplified spontaneous emission (ESASE) technique [3] was employed in order to produce two spikes in the electron peak current containing high-frequency peak current modulations (microbunching) inside them. This microbunching was essential for coherent radiation in the two short undulators located downstream. The first step of this approach included obtaining the longitudinal phase space with isolated bands in the energy as shown in Figure 1.

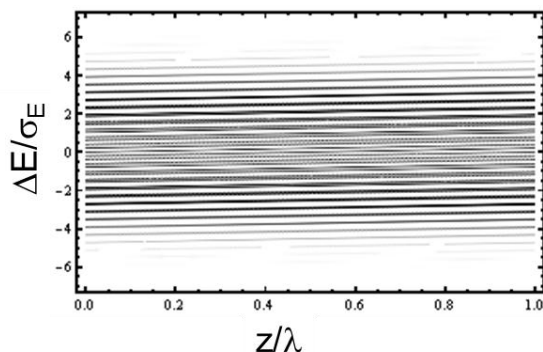


**Figure 1.** *The longitudinal phase space. The horizontal axis shows the electron's longitudinal coordinate normalized on the modulating laser wavelength. The vertical axis shows the electron's energy normalized on the rms energy spread.*

A typical distance between neighboring bands is 13.5 keV. Recently, it was noted [4] that for the electron beam parameters considered in [1], the intrabeam scattering (IBS) can induce an energy spread of the order of 7.5 keV when the electron bunch passes through an approximately 10-m-long lattice, a typical distance needed for conversion of the longitudinal phase space in Figure 1 to the longitudinal phase space with microbunching. Therefore, it is expected that the microbunching will be washed out by the IBS. In principle, spacing between the energy bands can be increased (and, thus, the impact of the IBS can be decreased) if a more powerful and shorter wavelength laser than that considered in [1] can be used in the process of laser manipulation of the electron beam leading to the appearance of longitudinal phase space with energy bands. However, currently it is not clear if such a laser can be developed and also if the projected improvement will be sufficient. Recognition of this situation motivated thinking about new ways for generating two-color ultra-short x-ray pulses with controlled time delay between them. One possibility is considered in this paper.

## II. Method

The following conditions were assumed to be essential for a new proposal: a) photon energies for the first and the second x-ray pulses can be independently chosen in a wide range, b) time delay between two x-ray pulses can vary in a wide range from zero to hundreds of femtoseconds and can be controlled with better than a femtosecond precision, c) each x-ray pulse should contain in excess of  $10^9$  photons.

To satisfy these requirements, we propose to use the scheme shown in Figure 2. This scheme is based on the idea of generation of ultra-short hard x-rays pulses first proposed in [5] and later adapted in [6] for generation of ultra-short soft x-rays pulses.

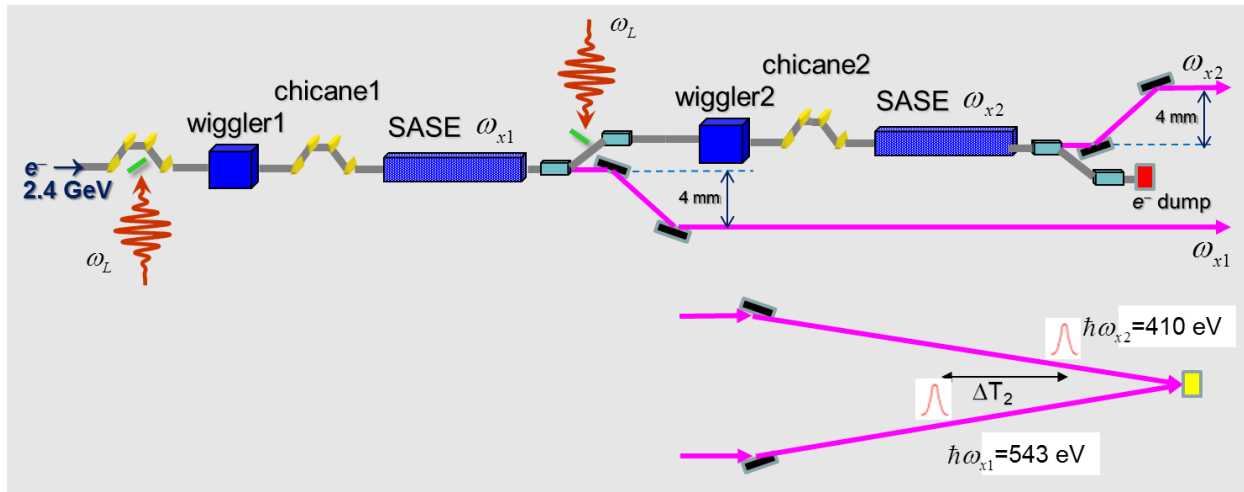


**Figure 2.** A schematic of the FEL system producing, in this example, one x-ray pulse with photon energy at the K-edge of the oxygen,  $\hbar\omega_{x1}$ , and one x-ray pulse with photon energy at the K-edge of nitrogen,  $\hbar\omega_{x2}$ , with a controlled time delay  $\Delta T_2$  between them.

The electron bunch with the electron energy of 2.4 GeV enters this scheme from the left. It passes a small magnetic chicane used to bypass a mirror and enters the first wiggler. At the same time the light pulse with active carrier-envelope phase stabilization and a carrier frequency  $\omega_L = 2\pi c / \lambda_L$ , where  $c$  is the speed of light and  $\lambda_L$  is the laser wavelength, enters the same wiggler. As noted later, it is beneficial for this scheme to use laser pulses with a relatively long wavelength of the order of 2  $\mu\text{m}$ . As shown in [7], such laser pulses can be obtained from a three-stage optical parametric chirped-pulse amplifier laser system. The specific system described in [7] produces carrier-envelope-phase-stable 15.7-fs (2-cycle) 740- $\mu\text{J}$  pulses at a 2.1- $\mu\text{m}$  carrier wavelength at a 1-kHz repetition rate. Using this laser with only 10% of the laser pulse energy, and choosing the wiggler with only two periods, and matching the wiggler period length (10 cm) and the peak magnetic field (1.63 T) for the efficient interaction of the electrons with the laser light with a 2.1- $\mu\text{m}$  carrier wavelength, one obtains energy modulation of electrons shown in Figure 3.

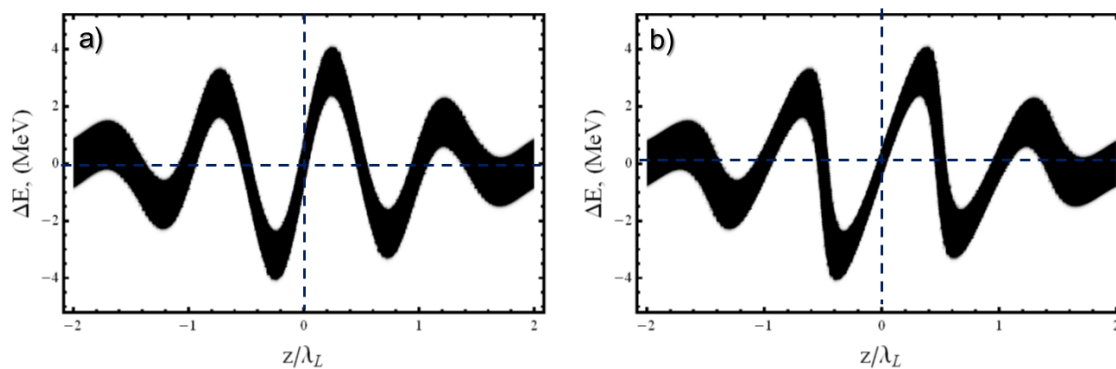


**Figure 3.** Energy modulation of electrons produced by a carrier-envelope-phase-stable 15.7-fs, 75- $\mu$ J laser pulse with 2.1- $\mu$ m carrier wavelength interacting with the electron bunch in the 2-period wiggler magnet. The width of the black curve is defined by the incoherent energy spread that in this case was chosen to be 200 keV. The horizontal axes show the distance along the electron bunch normalized on the laser wave length. Only a short fragment of the electron bunch is shown. a) Longitudinal phase space before the chicane1 in Figure 2, b) Longitudinal phase space after the chicane1 in Figure 2 with  $R_{56}=160$   $\mu$ m.

The peak-to-peak energy variation is approximately 7 MeV and the phase of the laser field is selected in such way that the electric field has a zero crossing when the center of the laser pulse reaches the center of the wiggler. In this case a large energy chirp is created for a short range of the electron bunch. Downstream of the wiggler in Figure 2 is the trimming chicane that can be used to modify the energy chirp if necessary. For example a shallower chirp shown in Figure 3a can be preferred for generation of a long wavelength x-rays. Finally we note that to the left and right of the main energy chirp there are two locations with similar large energy chirps going in the same direction as the main chirp. It is actually desirable to have these energy chirps much smaller than the central one. The difference in the magnitude of the chirp is largely defined by the laser pulse duration; this is why the laser pulses with shorter duration are preferred. If such pulses are not available or if better distinction between the main and side chirps is needed, then two laser pulses with different carrier wavelengths and two wigglers can be used. The electron beam interaction with these two pulses can increase the main chirp and decrease the side chirps at the same time. This is very similar to a technique that was previously explored in [8, 9] in order to increase the contrast of the attosecond x-ray pulses. For reader convenience Figure 4 show the magnitude of the peak-to-peak energy variation as a function of the laser pulse energy calculated, following the recipe developed in [10].

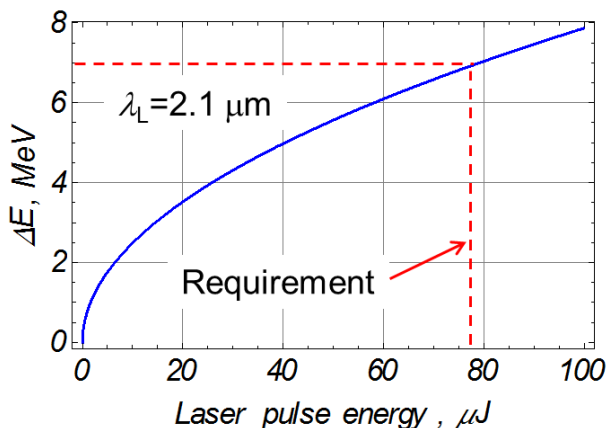


**Figure 4.** The magnitude of the peak-to-peak variation of energy modulation of the electrons produced in the interaction with a carrier-envelope-phase-stable 15.7-fs laser pulse with 2.1- $\mu\text{m}$  carrier wavelength as a function of the laser pulse energy.

The next box along the electron beam path in Figure 2 is the SASE undulator where the ultra-short x-ray pulse is created. Under normal conditions the energy chirp causes FEL gain degradation, but it can be prevented by means of the undulator tapering producing  $z$  dependence of the undulator parameter  $K$ . It can be understood by considering that the field experienced by the test electron was emitted by a second electron behind it at a retarded time. It is best when the carrier frequency of this field is in the FEL resonance with the test electron, e.g., when  $\gamma^2 = \lambda_u / 2\lambda_{x1} \times (1 + K^2 / 2)$ , where  $\lambda_u$  is the undulator period,  $\lambda_{x1}$  is the wavelength of the field,  $K$  is the undulator parameter, and  $\gamma$  is the relativistic factor. Therefore, the second electron with the energy offset can only emit a field with the right frequency if the undulator parameters are different at the retarded time. For large  $d\gamma/dt$  this requirement can be formulated with an approximate condition:  $d\gamma/cdt \times (\bar{\beta}_z - 1) \approx (d\gamma/dK) \times (dK/dz)$ , where  $\bar{\beta}_z$  is the electron longitudinal velocity averaged over the undulator period and normalized on  $c$ . From these considerations one can obtain [5, 6]:

$$\frac{d \ln K}{dz} = - \frac{\lambda_{x1}}{\lambda_u} \frac{1 + K^2 / 2}{K^2 / 2} \frac{d \ln \gamma}{cdt}. \quad (1)$$

Only a short slice of the electron bunch around the zero-crossing of the energy modulation in Figure 3 will produce a powerful FEL pulse when the undulator taper matches Eq. (1). The main unmodulated part of the electron bunch will suffer from the undulator taper and will have much reduced or nonexistent FEL gain. Figure 5, copied from Ref. [6], shows that, in fact, the calculated output signal is dominated only by one slice of the electron bunch. Typical pulse duration of the central peak is about 1-2 fs (FWHM) and typical peak power ranges up to 1 GW. Such a pulse contains over  $10^{10}$  photons and has a near Fourier-transform-limited time bandwidth product. It dominates the SASE radiation coming from the two side peaks (barely visible in Figure 5) plus spontaneous and SASE emission in the first harmonic from the rest of the electrons in the electron bunch (assuming the electron bunch length is less than 100 fs). The x-ray optics briefly discussed below can help to reinforce a good contrast, acting as the x-ray

collimation system and assisting in selection of only the main transverse mode of the FEL radiation.

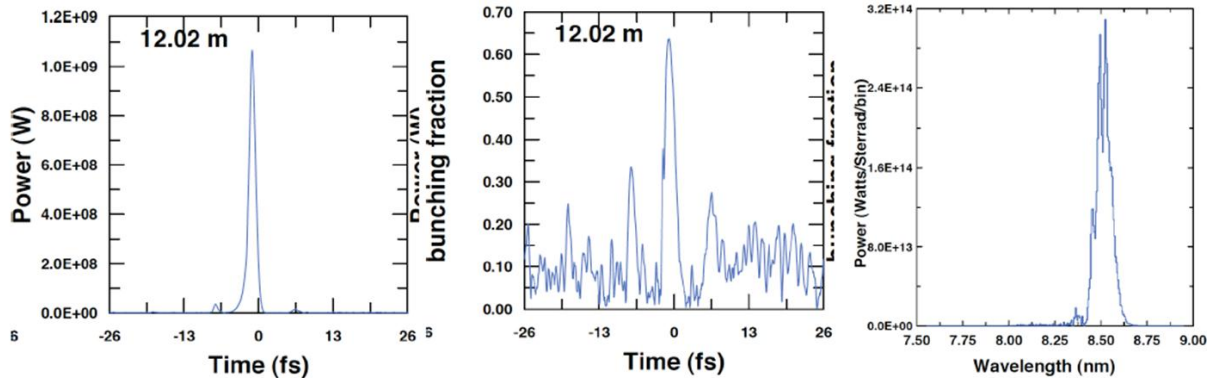


**Figure 5.** Instantaneous power, bunching, and on-axis far-field spectrum at undulator exit ( $z = 12$  m) for a SASE FEL resonant at the 8-nm x-ray wavelength (reproduced from Ref. [6]).

Slippage of the FEL radiation with respect to the electron bunch plays an important role in the above-described technique for generating ultra-short x-ray pulses. If the distance between two energy peaks defining the central energy chirp in Figure 1 is smaller than the projected slippage along the undulator that would be needed in order to reach saturation, then the FEL performance will suffer and the output power will drop. Thus, the longer laser wavelength is preferred in the case of generating soft x-ray pulses, as discussed in [6].

At the end of the FEL the electron beam path and the x-ray path are separated by using an achromatic dogleg-like magnetic lattice for the electron beam and a set of two x-ray mirrors for the soft x-ray radiation. As shown in Figure 6, mirrors are used at a small incidence angle in order to support a relatively wide bandwidth of ultra-short x-ray pulses. It also helps to cover a large range of x-ray photon energies with relatively high efficiency of transmission of the primary photon flux (see Figure 7).



**Figure 6.** A schematic of the soft x-ray take off mirror system used at the glancing incidence angle of  $1.5^\circ$  (not shown to scale).

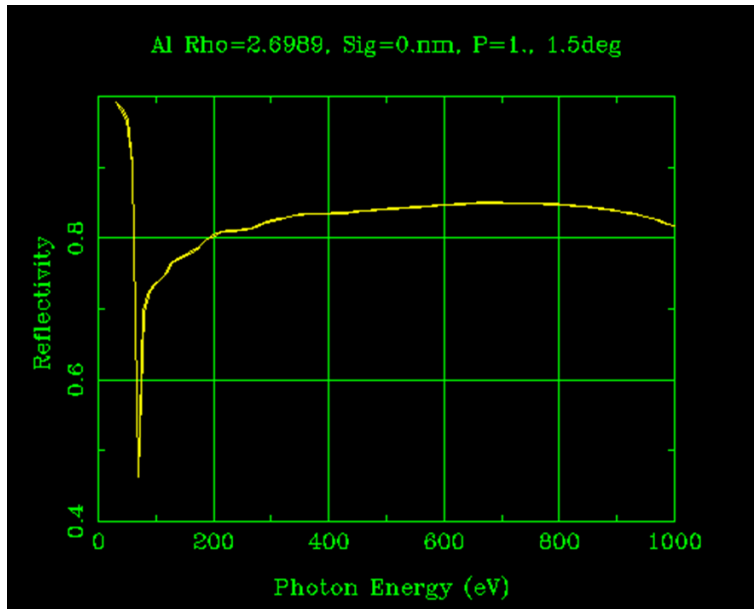


**Figure 7.** Aluminum mirror reflectivity versus photon energy for  $1.5^\circ$  glancing incidence angle [11].

The second part of the scheme shown in Figure 2 is essentially the same as the first part. The only difference is that the undulator is tuned for the FEL resonance at different photon energy. It is assumed that the electrons used in the second part are not much affected by the FEL process in the first undulator. It is also assumed that the laser pulse for the second part of the scheme comes from the same source as the laser pulse for the first part of the scheme. This ensures high-precision control over the time delay  $\Delta T_2$  between two x-ray pulses. The possible sources of timing variations/jitter are the variations of the path length for the laser pulse paths after the beam splitter, the electron bunch paths through the undulators, and the x-ray pulse paths through the x-ray optics that also includes combining two x-ray pulses on the sample at the end of the scheme. Under the assumption that the path length variations should only cause less than 10 attoseconds variation in time, previous estimates made for a similar system [12] produced the following requirements: a) the electron beam energy must be kept stable to approximately  $5 \times 10^{-5}$  precision, b) the magnitude of the fluctuations of the electron trajectory in the undulator should not exceed the electron beam size, and c) the magnetic field in each chicane magnet should not fluctuate more than 1%.

The minimum time delay between two laser pulses is approximately equal to two times the duration of the laser pulse. This is because one needs to avoid undesirable interference between two energy modulations if two laser pulses act too close in time. However, by setting the path lengths through the x-ray optics, one can compensate this delay and make sure that two x-ray pulses can arrive on the sample either simultaneously or with any predefined time delay regulated by adjusting  $\Delta T_1$ .

### III. Test Opportunity at LCLS

Figure 8 shows a proposed schematic of the above-described technique as applied to the LCLS. The CEP laser pulse enters through the BC2 and interacts with the electron bunch at 4.5 GeV in

the downstream wiggler magnet. This wiggler is appropriately tuned for the laser wavelength of 2.1  $\mu\text{m}$  (e.g., period  $\approx 30$  cm, peak magnetic field  $\approx 1.7$  T) and may also have enough flexibility to support interaction with the 0.8- $\mu\text{m}$ -wavelength laser (e.g., period  $\approx 30$  cm, peak magnetic field  $\approx 1.0$  T). Although the two-period wiggler is needed, the recommendation is to consider installation of a special wiggler that can support operation either with two periods or with a larger number of periods, e.g., ten periods. A wiggler with more periods will allow implementation of other FEL techniques not discussed in this proposal.

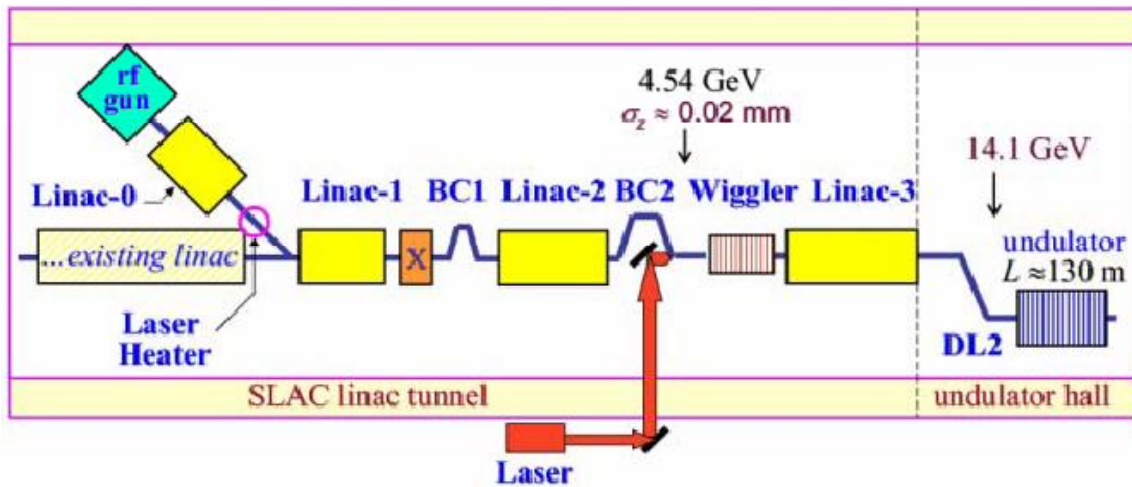


Figure 8. Schematic of the test set-up at the LCLS (not to scale).

The basic hardware system requirements for implementation of the technique are:

- Laser room in the klystron gallery above the linac, modulating laser system and laser light transport line to BC2,
- Modulating wiggler magnet satisfying above-described specifications,
- Diagnostics for the laser pulse e-beam overlap and for characterization of the laser e-beam interaction, and
- Small magnetic chicane before the FEL undulator for extended tunability of the technique.

#### IV. Conclusion

A scheme has been proposed for generation of two ultra-short x-ray pulses with different and adjustable photon energies using a single electron bunch for x-ray pump and x-ray probe experiments with a variable time delay between the first and second x-ray pulses. Each x-ray pulse contains in excess of  $10^{10}$  photons. The implementation of this scheme is based on the SASE FEL, which is a rather robust technique for soft x-ray wave lengths by today's standards. One drawback of this scheme compared to the previous proposal discussed in Ref. [1] is that the shortest duration of the x-ray pulses is limited only by 1-2 fs depending on the x-ray wavelength. Another drawback is the increased vulnerability of the timing jitter to variations in the electron beam, laser pulse, and x-ray pulse path lengths, which is simply a result of using much longer installations in some parts. On the positive side, the new scheme removes some limitations of the

former scheme, for example, allowing one to vary the time delay between two x-ray pulses beginning from zero or even a negative time delay. It also produces significantly more photons per pulse (e.g., in excess of  $10^{10}$  photons per pulse). Part of this is because the x-ray pulse is longer and part of it is because the FEL process (rather than coherent undulator radiation) is used to generate the x-ray pulses. The proposed scheme is not limited only to ultra-short x-ray pulses and can be used within the same basic set-up for a larger variety of FEL configurations.

Finally, here is a brief outline of the key technical components that will enable the above-discussed scheme to operate with an electron beam at 2.4-GeV electron beam energy:

- The laser system producing two carrier-envelope-phase-stable 15.7-fs (2-cycle) 70- $\mu$ J pulses at the 2.1- $\mu$ m carrier wavelength and laser light transfer lines. (A laser system with a shorter laser wavelength may also work for generation of x-rays with shorter than 8-nm wavelengths used in the proof-of-principle analysis in Ref. [6].)
- Two modulating wigglers, each with two wiggler periods of 10 cm length and peak magnetic field of 1.63 T.
- Two SASE FELs tunable in the range of photon energies defined by experimental needs.
- Two magnetic chicanes, one achromatic dogleg-like magnetic lattice, various diagnostics, broadband x-ray mirrors.

The repetition rate of this facility is defined by the maximum laser pulse repetition rate, which is currently limited to approximately 5 kHz, as may be extrapolated from the set of above-described parameters from the laser system discussed in Ref. [7]).

## Acknowledgments

The author benefitted from discussions with Paul Emma, Gregg Penn, Marco Venturini and other members of the NGLS team. The author is also thankful to John Byrd and John Corlett for support during his stay in LBNL. This work was supported by the U. S. Department of Energy, Office of Science, under Contract No. DE-AC02-06CH11357.

---

<sup>1</sup> A. Zholents and G. Penn, Nucl. Instrum. Methods A **612**, 254 (2010).

<sup>2</sup> G. Stupakov, Phys. Rev. Lett. **102**, 074801 (2009).

<sup>3</sup> A. Zholents, Phys. Rev. Spec. Topics Accel. Beams **8**, 040701 (2005).

<sup>4</sup> G. Penn, private communication.

<sup>5</sup> E.L. Saldin, E.A. Schneidmiller, M.V. Yurkov, Phys. Rev. Spec. Topics Accel. Beams **9**, 050702 (2006).

<sup>6</sup> W.M. Fawley, Workshop on Frontiers in FEL Physics, <http://www.inf.infn.it/conference/elba07/> .

<sup>7</sup> Xun Gu *et al.*, Optics Express **17**(1), 62 (2009).

<sup>8</sup> A. Zholents and G. Penn, Phys. Rev. ST Accel. Beams **8**, 050704 (2005).

<sup>9</sup> Y. Ding, Z. Huang, D. Ratner, P. Bucksbaum and H. Merdji, Phys. Rev. ST Accel. Beams **12**, 060703 (2009).

<sup>10</sup> A. Zholents, K. Holldack, Free-Electron Laser Conference, FEL06, Berlin, Germany, (2006); LBNL-61515.

<sup>11</sup> Calculated using interactive web site [http://henke.lbl.gov/optical\\_constants/mirror2.html](http://henke.lbl.gov/optical_constants/mirror2.html)

<sup>12</sup> A. Zholents, W. Fawley, Phys. Rev. Lett. **92**, 224801 (2004).